An Alternative Sea Level Pressure Reduction and a Statistical Comparison of Geostrophic Wind Estimates with Observed Surface Winds

STANLEY G. BENJAMIN* AND PATRICIA A. MILLER

NOAA Environmental Research Laboratories, Forecast Systems Laboratory, Program for Regional Observing and Forecasting Services (PROFS), Boulder, Colorado

(Manuscript received 5 January 1990, in final form 9 April 1990)

ABSTRACT

A method for station or grid point reduction of surface pressure to sea level or some other level is presented that shows improvement over the standard reduction method in the western United States. This method (MAPS SLP—Mesoscale Analysis and Prediction System sea level pressure) uses the 700 hPa temperature to estimate an "effective" surface temperature from which the temperature of the hypothetical layer beneath the ground is estimated. The use of this "effective" temperature instead of the observed surface temperature is responsible for the improved reduction since it varies more smoothly over space and time and is more representative of the temperature variation found above the boundary layer.

The MAPS SLP reduction was compared with the standard reduction and altimeter setting reduction in statistical comparisons of geostrophic wind estimates with observed winds and in a case study. A 21-month comparison between geostrophic and observed winds was made over different geographical regions, times of day, rotation angles and seasons. The results showed that the MAPS SLP reduction performed better than the standard reduction in the western United States, but not in other regions with generally low elevation. In general, the correlation between sea level geostrophic winds and observed winds was found to be dependent on the Froude number. A statistical comparison using a smaller sample between MAPS SLP and the Sangster geostrophic wind, which is not a station reduction, showed similar skill over the western United States. The case study also showed that the pattern over the western United States was more coherent and less anomalous with MAPS SLP that with the other reductions.

1. Introduction

The sea level pressure analysis is widely used by forecasters to estimate the pressure gradient force at the surface and the strength and direction of surface flow when wind observations are not available. If surface wind observations are available, the sea level pressure field is commonly used to estimate the ageostrophy of those winds. These estimates are often made even over high elevation regions because surface analyses can be made with greater spatial and temporal resolution than analyses at 850 or 700 hPa.

Over higher terrain, sea level pressure is calculated by reducing surface pressure to zero elevation. As many have pointed out, in particular, Sangster (1960, 1987), the reduction often produces sea level pressure fields that are misleading in high elevation areas because an assumption is made in the reduction algorithm concerning the temperature of the fictitious air layer between the surface and sea level. This assumption, applied at different locations, may produce fictitious baroclinity in the subsurface layer and result in errors in the estimate of horizontal surface pressure gradient.

An alternative method of reducing surface pressure to sea level is presented which does not eliminate these errors but gives smaller errors than those given by the conventional reduction. The alternative reduction is tested within a surface analysis package described by Miller and Benjamin (1988). To validate the alternative reduction method, observed surface winds are statistically compared with sea level geostrophic winds from different reductions, including the new one, which allowing for variation in 1) geographical region, 2) season, 3) time of day and 4) cross-isobar angle.

This comparison is made since observed winds are an *independent* source of information that are usually well correlated with the geostrophic wind. The degree of correlation is limited, or course, by various ageostrophic effects including isallobaric and advective influences on the larger scale and local influences usually related to the surface. It is also limited by errors induced by baroclinity beneath the surface when sea level pressure gradient is used to estimate surface winds, as we have done in this paper. This evaluation of different pressure reductions is performed over a large data set rather than just a few case studies. The resulting statistics support the hypothesis that the alternative reduction is an improvement over other reductions; they

* Also affiliated with the National Center for Atmospheric Research, which is sponsored by the National Science Foundation.

Corresponding author address: Dr. Stanley G. Benjamin, NOAA/ERL/FSL, R/E/FS2, 325 Broadway, Boulder, CO 80303

also show that the correlation between observed surface winds and sea level geostrophic winds decreases for changes in region/time of day/season that are consistent with a decrease in the Froude number.

2. Sea level reduction methods

All methods of pressure reduction are based on an equation derived from the hydrostatic and hypsometric equations:

$$p_{SL} = p_{sfc}\left(\frac{T_0 + \gamma z}{T_0}\right)^{g/R\gamma} \quad (1)$$

where p_{SL} is the pressure reduced to sea level, p_{sfc} is the surface pressure, T_0 is a temperature assumed to be valid at the surface (but not necessarily the observed surface temperature), γ is a temperature lapse rate (constant in the horizontal and vertial), z is the surface elevation, g is gravity, and R is the gas constant. To account for moisture effects, virtual temperature should be used with the gas constant for dry air. The derivation of an equation very similar to this is shown in Wallace and Hobbs (1977, p. 60–61).

Here three methods of reduction are compared: the standard method (standard SLP), the altimeter method (ALT), and the alternative method, developed as part of the Mesoscale Analysis and Prediction System (MAPS) at PROFS, designated as MAPS SLP. All three methods use the Standard Atmosphere lapse rate (γ_s = 6.5 K / 1000 m) to estimated increase of temperature from the surface to sea level through the below-ground column. The primary difference is that the methods use different estimates of the surface temperature from which to start the hydrostatic integration downward toward sea level.

The standard SLP reduction [Manual of Barometry 1963 (p. 7–5); Saucier 1955 (p. 58)] estimates this temperature as:

$$T_0 = \frac{T_{sfc}(\text{current}) + T_{sfc}(12\text{ h previous})}{2} \quad (2)$$

where T_{sfc} is an observed surface temperature. Use of the mean surface temperature is an attempt to remove the influence of the diurnal temperature wave on the reduction. Standard SLP has an additional "plateau" correction for stations at elevations higher than 1000 feet, which has the result of minimizing variations of annual mean SLP values.

The altimeter setting (ALT) uses the Standard Atmosphere to estimate the fictitious atmospheric mass between surface and sea level,

$$T_0 = T_{Stand.\ Atm.}(z). \quad (3)$$

The observed surface pressure thus may be recovered easily from the reported altimeter setting. A correction of 0.3 hPa is subtracted to allow for a mean cockpit height of 3 m above the runway. There is no seasonal adjustment in the Standard Atmosphere temperature.

The MAPS SLP reduction estimates the surface temperature used in reduction from the 700 hPa temperature reduced by the standard lapse rate (γ_s) to the surface elevation,

$$T_0 = T_{700}\left(\frac{p_{sfc}}{700}\right)^{R\gamma_s/g}. \quad (4)$$

The 700 hPa level was chosen as the lowest mandatory level which is usually not strongly influenced by diurnal effects. In practice, at PROFS, gridded forecast data at 700 hPa from the Nested Grid Model (NGM) are interpolated in space to the station location and in time to the observation time from 6 h frequency output from the latest NGM run (run every 12 h). This does make the MAPS SLP reduction model dependent. The advantages of MAPS SLP are that it is free from diurnal influence and local influence (instead using a reference level temperature that is regionally appropriate but smoothly varies in time and space), it uses station data directly and it is easy to calculate. It is based on altimeter setting, which can be easily converted into the surface "station" pressure p_{sfc} [using Eqs. (1) and (3)] and is reported at about 25% more stations over the United States than standard SLP. Moreover, as additional surface stations (ASOS—Automated Surface Observation System) are added over the next few years, the MAPS SLP reduction may be used with them immediately, whereas use of standard SLP will require the calculation of a "plateau correction" for each station.

In general, use of a surface temperature that is too high for pressure reduction at a high elevation station will result in SLP values that are too low and temperatures that are too low will produce SLP values that are too high. Despite the mean temperature and plateau correction used in the standard SLP reduction, local effects such as cold air pooling in valleys often distort standard SLP values reported in the western United States. The passage of a front at a high elevation station results in an unrealistic jump in the standard SLP value, since the temperature used to reduce the surface pressure has suddenly changed. The standard SLP pressure gradient over elevated but flat terrain such as the western plains of the United States and Canada is exaggerated behind cold fronts for the same reason. Some of these effects have been documented by Sangster (1960, 1987), Garratt (1984), and Saucier (1955). Saucier stated (p. 64) that the primary reason for inconsistency in reduced sea level pressure patterns over elevated terrain is that surface temperatures are unrepresentative of the horizontal pattern of temperature in the free atmosphere owing to the irregular character of the earth's surface, including orography, exposure, soil cover, etc. Saucier also stated that "The most suitable temperature for reduction of pressure to sea level is

not surface temperature but temperature at some height beyond the immediate masking effects by the surface." This requirement is met by using gridded 700 hPa temperature data as a basis for reduction.

For regional domains, the reduction problem can be minimized by reducing to the mean elevation for that domain rather than to sea level (e.g., Mass and Dempsey 1985; Danard 1989). A regional surface analysis centered on Colorado developed at PROFS, for example, uses the 700 hPa temperature technique but reduces to an elevation of 1500 m. For domains such as the contiguous United States, an assumption must be made about the temperature of the subsurface layer all the way down to sea level.

Another approach to estimating the surface pressure gradient has been to estimate the local gradient in a sigma coordinate system relative to a smoothed topography field, and then to solve a resulting Poisson equation for a stream function from which the geostrophic wind can be calculated. Sangster (1960, 1987) and Pielke and Cram (1987; see also Cram and Pielke 1989) both used techniques based on this idea. The Sangster surface geostrophic wind has been in use within the National Weather Service for several years. Pielke and Cram applied their technique to solving for a surface geostrophic wind from three-dimensional data, for example, from model initial fields or forecasts. Davies-Jones (1988) demonstrated that the Sangster and Pielke and Cram techniques are essentially the same.

The alternative method described in this paper is different from these approaches and similar to the conventional reduction in that a pressure reduction is produced at individual stations, which may then be directly analyzed rather than determined as a solution to a Poisson equation requiring lateral boundary conditions.

3. Collection and treatment of data

Surface wind observations and geostrophic wind components, bicubically interpolated to the observation sites, were collected at 0000 and 1200 UTC at stations within five distinct geographic regions with different terrain characteristics (Fig. 1). These data were collected during seven seasons between December 1987 and August 1989 (winter: December–February; spring: March–May; summer: June–August; fall: September–November). The geostrophic winds were calculated from analyzed fields of sea level pressure observations using three reduction schemes. The three sea level pressures are MAPS SLP, standard SLP, and altimeter setting (ALT). Nine rotation angles were used to account for surface friction in the geostrophic winds: −15°, 0°, 15°, 30°, 45°, 60°, 75°, 90° and 105°. All observations of wind and reduced pressures were quality-controlled through a "buddy check" based upon optimum interpolation (Gandin 1963). The pressures

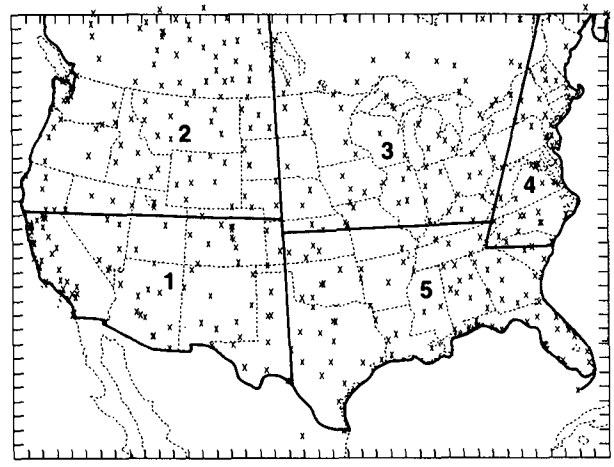

FIG. 1. The geographical regions used for statistical calculations and listed in Table 1. Stations used in each region are shown with an ×.

were analyzed to a 42 × 32 grid at a 111-km spacing covering the contiguous United States as described by Miller and Benjamin (1988). In this system, a new analysis is calculated hourly; the previous hour's analysis serves as a background for the current hour's analysis and quality control. Geostrophic winds for each reduction were calculated using the map scale factor appropriate at each grid point.

Two measures were used to judge the statistical comparisons between geostrophic winds and observed surface winds: *correlation coefficient* and *slope of the regression line.* Linear correlation coefficients measure the goodness of fit of the data to a linear equation. A perfect correlation of one indicates that a straight line totally explains the relationship between two variables. For this comparison, this means that if a scatter diagram were plotted with the (rotated) geostrophic wind component on the X coordinate and the observed wind component on the Y coordinate, then all the points of the scatter diagram would lie on a line. A perfect correlation does not indicate that the geostrophic wind components *equal* the observed wind components; it just indicates that there is a perfect linear relationship between the two variables.

For a sample size of 6000 (typical for one region and one season), the 95% confidence limits for a correlation coefficient of 0.35 calculated from Fisher's z transformation are 0.33 and 0.37, or ±0.02. This 95% confidence interval of 0.02 can be applied to all the regional/seasonal correlation coefficient comparisons shown in this paper.

To see how close the geostrophic and observed components tend to be, the slope of the regression line of Y (the observed winds) on X (the geostrophic winds) was also calculated. A slope of one indicates that the geostrophic wind components are matching the observed wind components, a slope of zero indicates that

an observed wind component can be associated with the full range of geostrophic wind components (a most undesirable situation) and a slope of 0.5 means that the observed wind components are, on the average, half those of the geostrophic wind. The slopes were calculated, as were the correlation coefficients, for four seasons, five geographic regions, two times of day and nine rotation angles.

Sangster geostrophic winds derived from MAPS quality-controlled surface observations were added to the data set for a 30-day period in August–September 1989.

4. Results of statistical comparisons between observed and geostrophic winds at the surface

As this study began, we were aware that surface observations become increasingly susceptible to local effects at nighttime and near mountains. This problem of representativeness in surface observations is well known and is dealt with at some length by Saucier (1955, p. 295–301). The variation of correlation between geostrophic and observed surface winds over season, time of day, and region appears to be strongly related to nocturnal inversions and to local topographical effects. In the following discussion, the Froude number (e.g., Gill 1982, p. 150) is used as a unifying concept for explaining these variations. The Froude number is defined as:

$$\mathrm{Fr} = \frac{U}{NH}. \tag{5}$$

where U is the wind speed, N is the Brunt-Väisälä frequency (stability),

$$N = \left(\frac{g}{\theta}\frac{\partial\theta}{\partial z}\right)^{1/2},$$

θ is the potential temperature, and H is the characteristic height of the topographical barrier.

The Froude number measures the extent to which stratification slows down parcels as they ascend the upwind side of a mountain (Pierrehumbert 1986). Blocking and other topographical effects are observed with $\mathrm{Fr} < 1$. McGinley (1984) used the Froude number within a constraint for variational analysis of flow around mountains.

a. Comparison of reduction methods

First, correlation coefficients between observed and geostrophic winds are examined for the different reductions tested. In a sense, we are testing different sea level geostrophic wind estimates as predictors of observed surface wind; using the correlation coefficient as a goodness-of-fit measure. Figures 2a–c shows correlation coefficients by season for each of the five geographic regions. Each point in this figure represents the maximum correlation coefficient achieved by each reduction method over the nine rotation angles listed in section 3. The rotation angle with highest correlation coefficient could (and did) vary among the reduction methods.

The largest differences between reductions occur in Region 1 (southwestern United States) and to a lesser extent in Regions 2 (northwest) and 5 (south central/southeast). In Region 1, the MAPS SLP reduction has the highest correlation with the observed wind, especially at 0000 UTC, for all three variables (u, v, and wind magnitude). In other regions, the differences in correlation are smaller, but the ALT reduction often shows much lower correlations, particularly in summer. This result is predictable since the use of the Standard Atmosphere (15°C at 1013.25 hPa and decreasing with increasing elevation) in the ALT reduction is least appropriate over the western United States in summer. The MAPS SLP and standard SLP reductions perform similarly east of the Rockies by the measure of correlation coefficient, although SLP has a slight edge in Regions 4 and 5. Since these regions are generally quite close to sea level (Table 1) and reduction differences should be very small, this behavior is attributed to the increased smoothness of the standard SLP analysis, which uses about 20% fewer observations than the MAPS SLP or ALT analyses. Thus, observed winds would correlate better with the large-scale pressure gradient than with the gradient on smaller scales, which changes more rapidly and is likely to have larger isallobaric effects.

To provide a better visual sense of the difference in correlation coefficients and slopes in Region 1 (southwest), scatter diagrams of observed/geostrophic pairs are presented in Fig. 3. These pairs, for the u component in summer 1988 with zero rotation, show that the largest and apparently most unrealistic geostrophic components occur with the ALT reduction (up to 60 m s^{-1}), followed by the standard SLP reduction. The range of geostrophic winds matches the range of the observed winds most closely with the MAPS SLP reduction. The correlation coefficients correspondingly increase from ALT (0.05) to standard SLP (0.16) to MAPS SLP (0.22) for zero rotation.

In general, larger differences between reductions occur at 0000 UTC than at 1200 UTC and in the western regions than in eastern ones. At 1200 UTC, winds are more likely to be light and variable beneath the nocturnal inversion and subject to local effects, in which case no estimate of surface geostrophic wind can correlate well with observed surface winds. At 0000 UTC, there should be a greater "potential" for high correlation between geostrophic winds and observed surface winds because of vertical mixing and lower stability; this potential is only evident in the statistics in Region 1 (Figs. 2a, 2b). The regional effect occurs because higher terrain magnifies errors in reduction methods. Where there are differences between reductions, MAPS

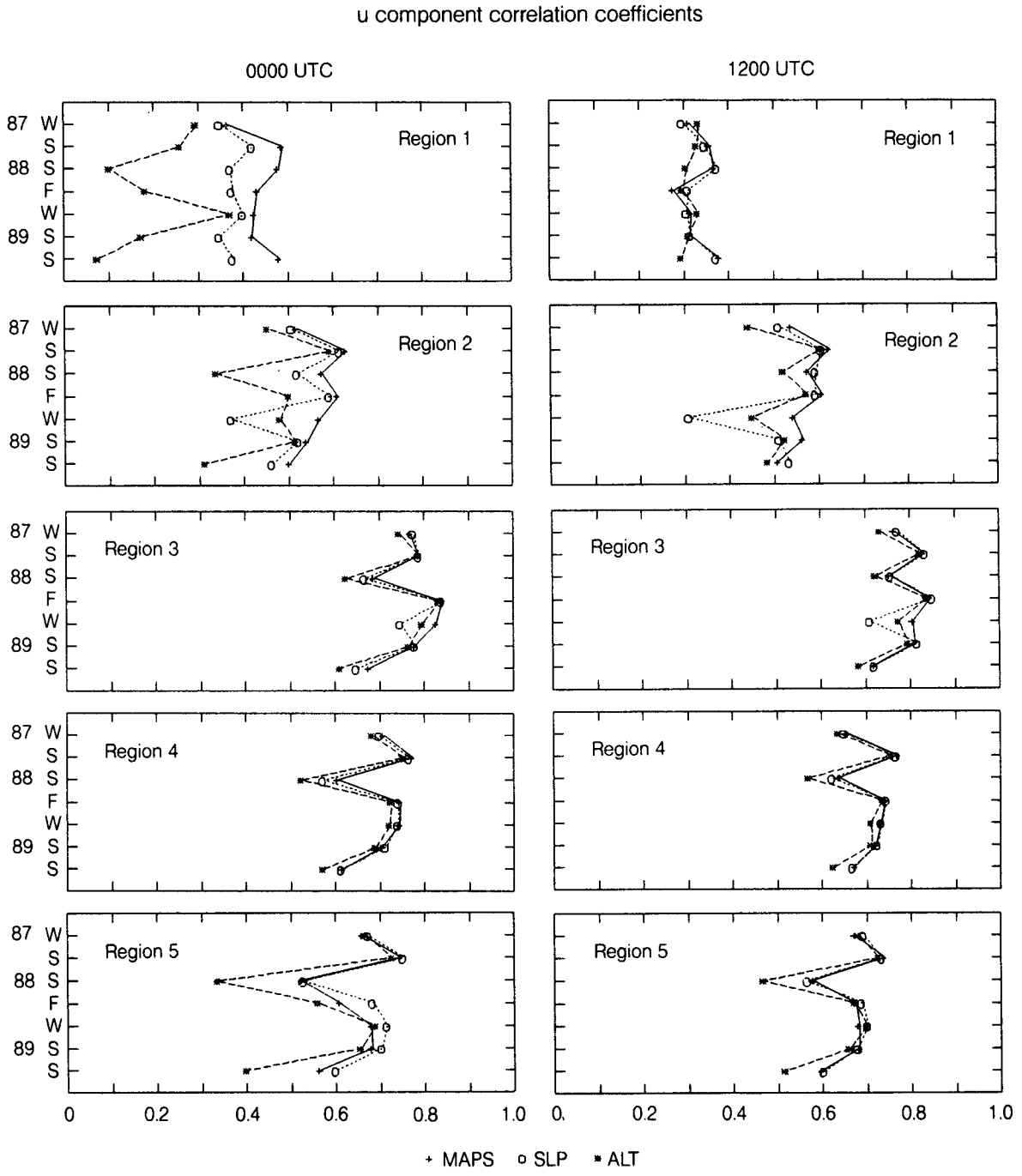

FIG. 2. Correlation coefficients between observed and geostrophic winds in different seasons, for different reduction methods. Coefficients are stratified by season. Coefficients plotted are the maximum values over all rotation angles: a) for u component relative to grid, b) for v component relative to grid, c) for wind magnitude.

SLP generally has the highest correlation, followed by standard SLP, and then by ALT.

The slopes of regression (not shown), representing the mean ratio between surface observed wind and geostrophic wind, also indicate that MAPS SLP provides some improvement in the southwestern United States but makes little difference elsewhere. The slopes generally show somewhat less variation with reduction method than the correlation coefficients. They increased from 0.01 (nearly horizontal line of regression) for ALT to 0.05 for standard SLP to 0.10 for MAPS SLP in Fig. 3 (u component with zero rotation for

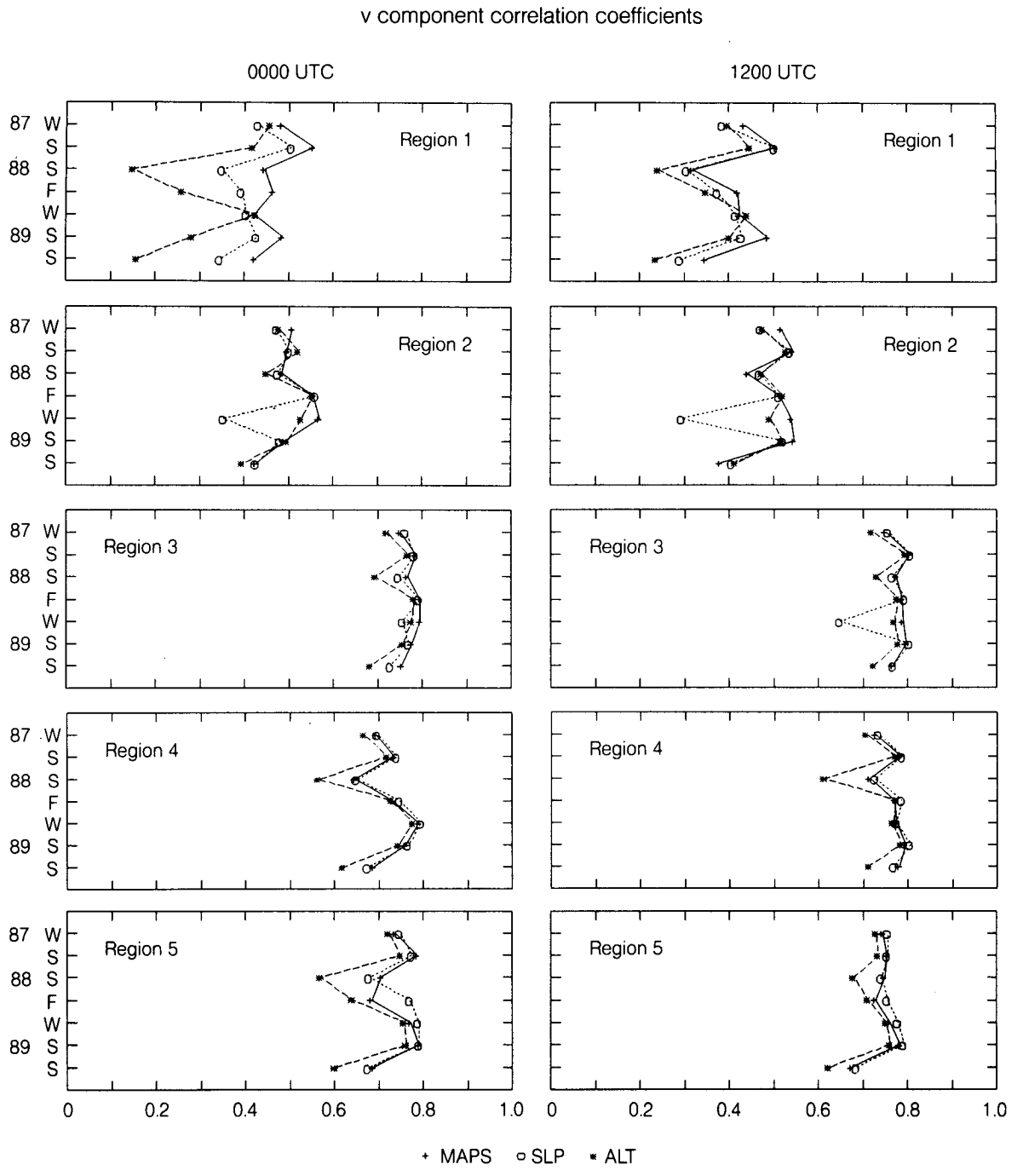

FIG. 2. (*Continued*)

Region 1 in summer). The slopes were very small when the entire sample was used but increased when only stronger winds were used (sec. 4.6).

The largest correlations and slopes closer to one would be expected over *flatter* terrain. Larger *differences* among reduction methods would be expected over *higher* terrain. This is, in fact, what occurred. The mean station elevation (Table 1) over which reduction occurs is much smaller east of the Rockies and is smaller in Region 2 (northwest) than in Region 1 (southwest). The MAPS SLP reduction showed the greatest improvement in Region 1 and somewhat less

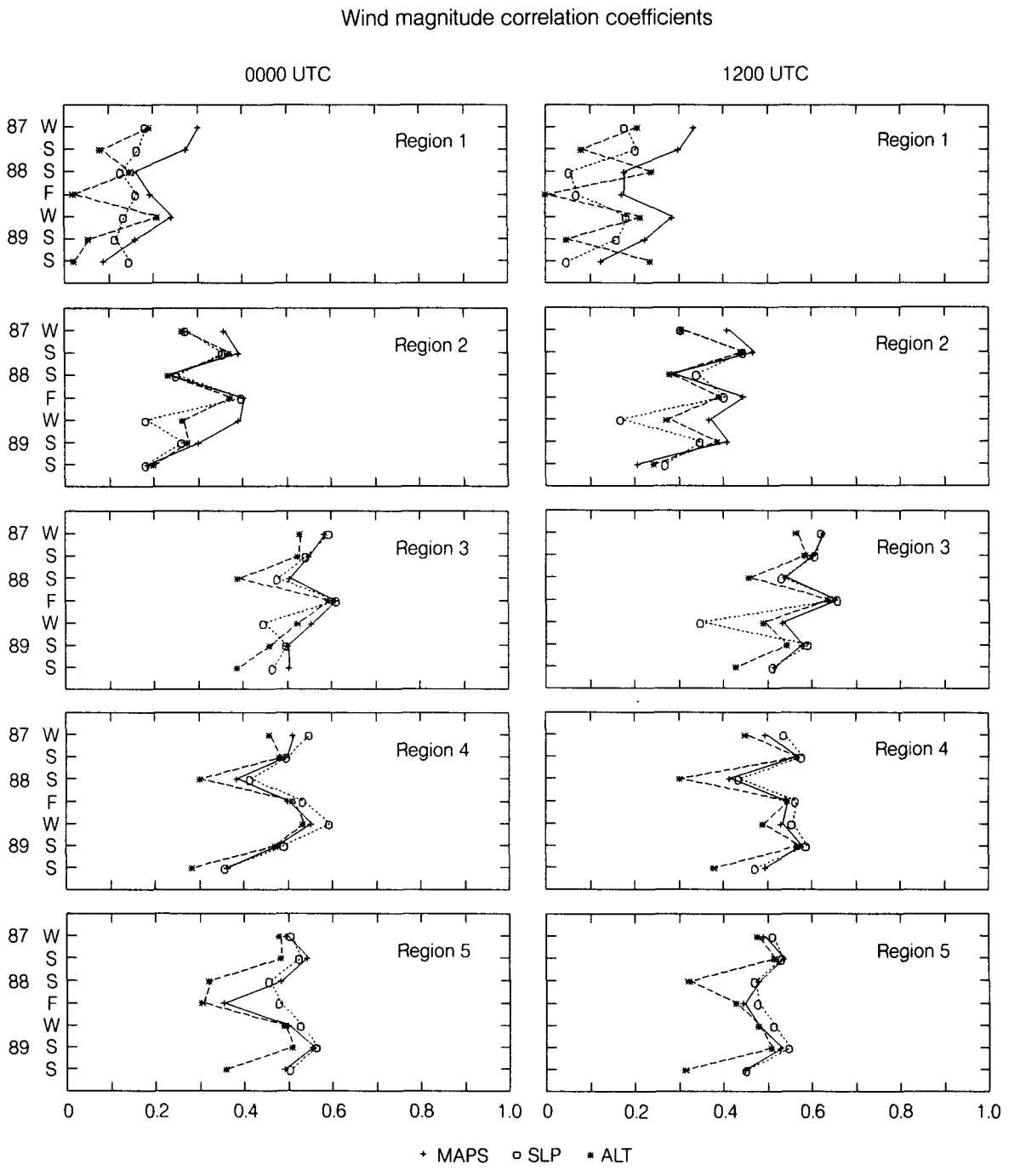

FIG. 2. (*Continued*)

in Region 2; little difference between reduction methods occurred in other regions where the correlations and slopes were much higher overall.

b. Seasonal variations

On the whole, there is some tendency for higher correlations (less scatter) during spring and fall evident in Fig. 2, and the lowest correlations tend to occur during summer. This tendency is found in all regions and at both 1200 and 0000 UTC.

We have two hypotheses concerning this behavior. The first is that the low-level Froude number tends to be at a maximum during the transition seasons and at a minimum during summer. This seasonal variation

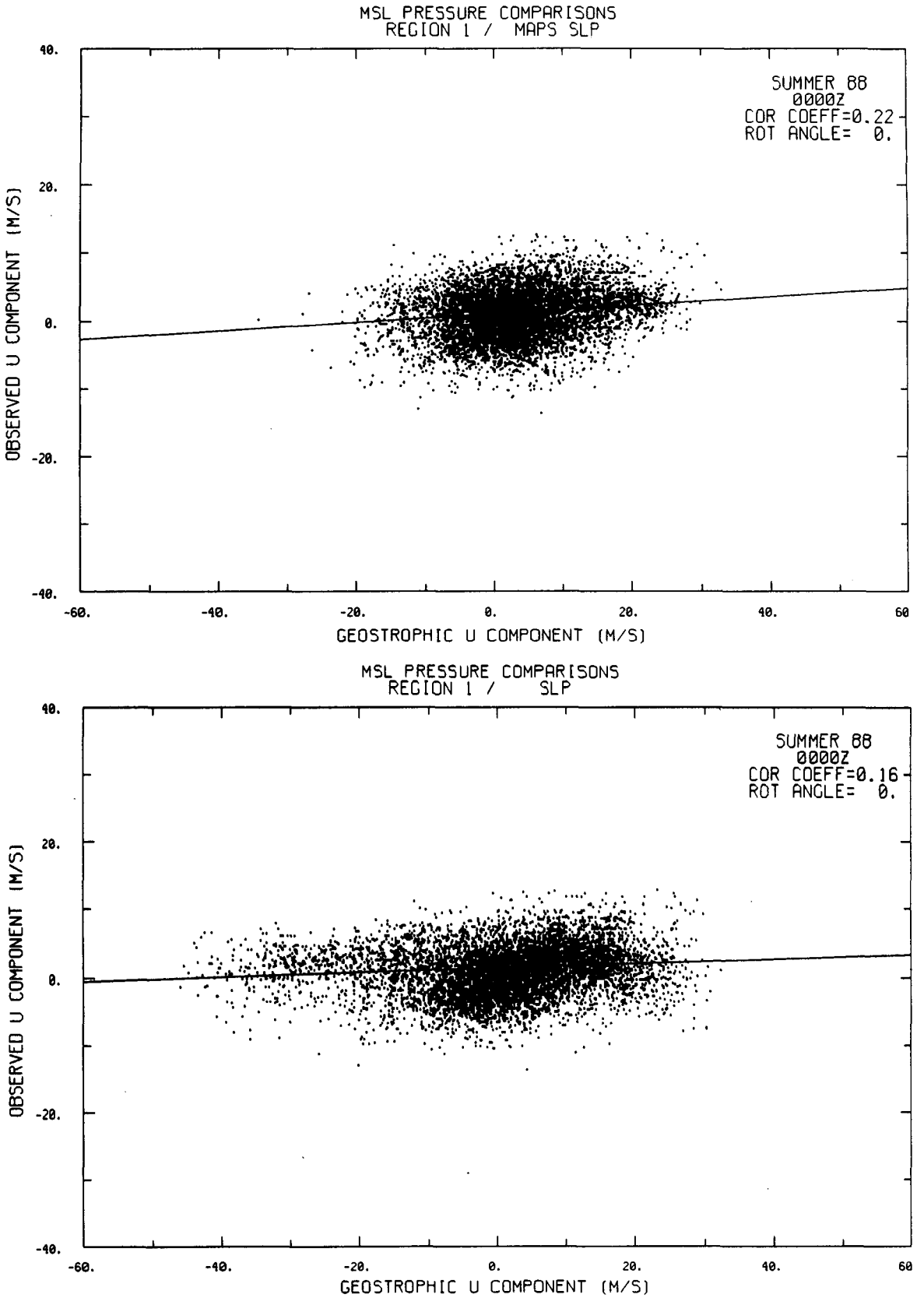

FIG. 3. Scatter diagrams for observed versus geostrophic u components during summer 1988 at 0000 UTC for rotation angle = 0°. Each point represents a single station on a particular day at 0000 UTC during that period. a) MAPS SLP, b) standard SLP, c) ALT.

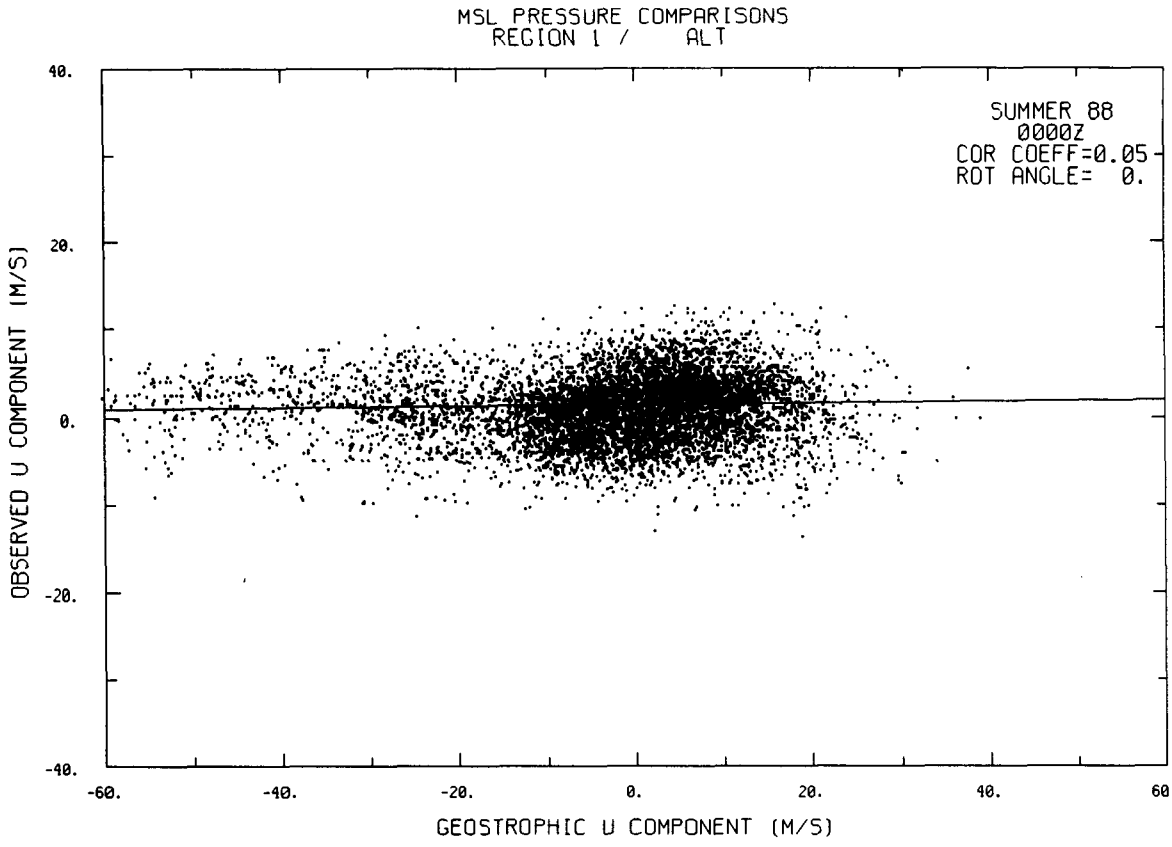

FIG. 3. (*Continued*)

of the Froude number, we hypothesize, would occur in middle latitudes because the mean wind speed is relatively high during transitional seasons while the low-level stability is frequently weak. Thus, the sensitivity of surface flow to local effects would be maximized in summer and in winter.

To investigate this Froude number hypothesis, Froude numbers from NGM analysis gridded data were calculated by region (at the locations shown in Fig. 1) and by time of day for the first 12-month period used for comparisons of geostrophic and observed winds. The Froude number [Eq. (5)] was calculated using 850 hPa winds as U, 700 hPa and 850 hPa temperatures for N, and the terrain standard deviation within a 111-km grid area (Fig. 4) for H. The results of these calculations (Fig. 5) partially confirmed this hypothesis, showing that Froude numbers were generally at a minimum during summer and at a maximum during spring, although not at a maximum during fall. In summer at 1200 UTC for individual stations using this NGM data set, the mean Froude number in Region 1 (southwest) was a relatively low value of about two. Figure 6 shows that both 850 hPa winds (U) and 700–850 hPa inverse stability ($1/N$) were equal or slightly higher in spring than in fall leading to a maximum in the Froude number and a minimum in local effects on surface flow in spring. As might be expected, winds were strongest in winter but their effect on the Froude number was more than offset by the increased stability in winter.

The second hypothesis is that the standard lapse rate assumption, used in all reduction methods, is more accurate in transition seasons. Therefore, the geostrophic wind estimates will also be more accurate then and less so in summer when the standard lapse rate is too stable and in winter when it is too unstable. This may help to explain the relatively high correlations in the fall statistics.

TABLE 1. Mean station elevation and terrain standard deviation for five geographical regions.

Region	Location	Mean station elevation (m)	Mean station terrain standard deviation (m)
1	Southwest	877	278
2	Northwest	799	203
3	North central	285	55
4	Northeast	112	65
5	South central/southeast	151	39

c. *Diurnal variations*

Larger correlations and slopes are found at 0000 UTC than at 1200 UTC in Region 1 and, to a small extent, in Region 2 (western United States). This diurnal variation is difficult to find in Regions 3, 4, and 5 (north central, northeast, and south central/southeast). A diurnal variation should be expected because of nighttime decoupling of the boundary layer from the free atmosphere. We suggest two reasons for the variation of diurnal influence with region. First, although conditions are generally more stable over the United States at 1200 UTC than at 0000 UTC, they are slightly less so over the eastern United States where synoptic times do not coincide so well with the times of surface temperature maxima/minima. Thus, the sample times are not positioned to capture diurnal variations in eastern regions. The NGM data also show a much stronger diurnal variation of the Froude number in the western regions than in the east (Fig. 5). Second, since topographical variations (Fig. 4 and Table 1) are much more widespread in the western two regions than in those to the east, the Froude number will be smaller in the western regions and local topographical effects will be greater, given equal mean wind speed and stability. When the Froude number is larger, the maximum possible correlation between "perfect" geostrophic and observed surface winds is increased. Thus, the correlations in Region 1 (southwest, Fig. 2) at 1200 UTC are strongly limited by local effects; at 0000 UTC, the MAPS SLP is able to show a greater improvement over the other reductions due to the greater potential for higher correlations at this time of day.

d. *Regional variations*

The lowest correlations and slopes occur in regions 1 and 2 (western United States). Region 1, which has the greatest terrain variations, also shows the lowest correlations (0.3–0.5 for u and v components) and slopes (0.1–0.25). Region 3 (north central) has the

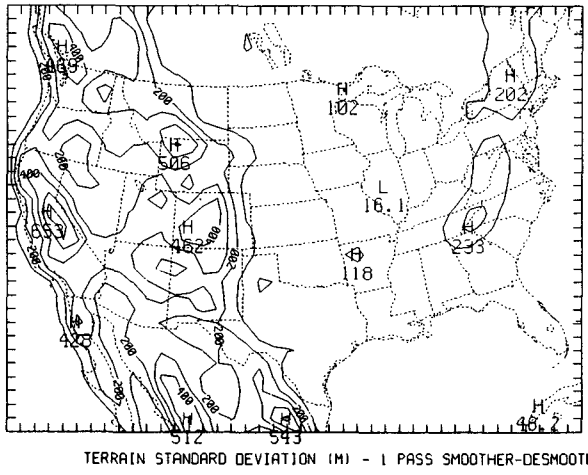

FIG. 4. Elevation standard deviation calculated from five-minute terrain data. The standard deviation was calculated over 111-km squares; 10 × 10 points were used in each square.

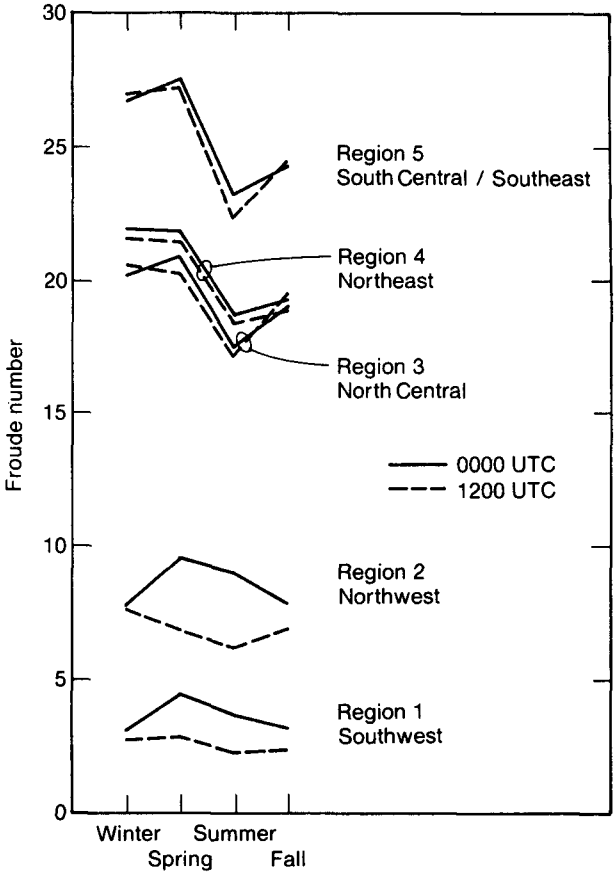

FIG. 5. Mean Froude number calculated from NGM analyses of 850 hPa winds and temperature and 700 hPa temperature. Solid lines are for 0000 UTC and dashed lines are for 1200 UTC. The values are calculated at the station locations shown in Fig. 1. The period December 1987–December 1988 was used for these calculations.

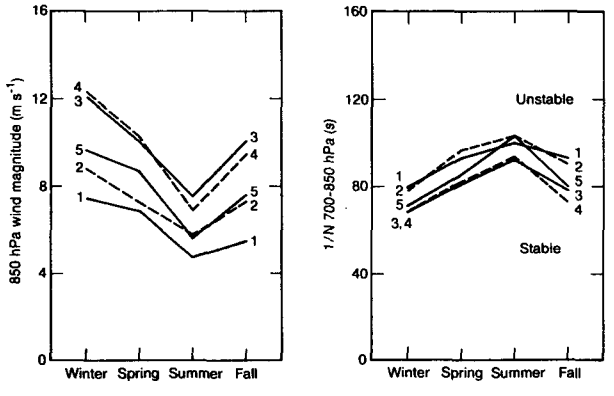

FIG. 6. Mean 850 hPa wind magnitude and 700–850 hPa inverse stability from NGM analyses. Region numbers are shown by each line; odd region numbers are solid and even region numbers are dashed. Values were calculated for station locations shown in Fig. 1.

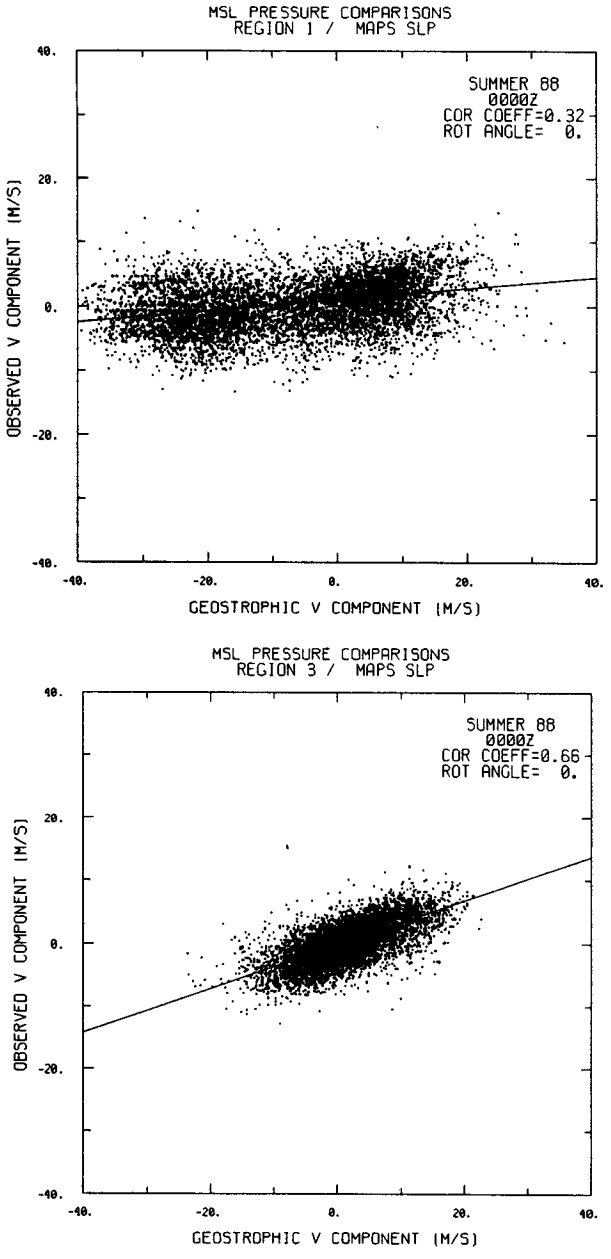

FIG. 7. Scatter diagrams for v components during summer 1988 at 0000 UTC. a) Region 1—southwestern United States, b)Region 3—north central United States.

highest correlations (0.7–0.85) and slopes (0.3–0.4), possibly because it is generally flat and contains no water influence except the Great Lakes. Regions 4 and 5 both have a large percentage of coastal area where sea/land breezes are influential, and Region 4 (northeast) also includes the Appalachian Mountains. Overall, the correlations and slopes are smallest where terrain variations are largest (Fig. 4), but marine influence may also cause local circulations which cause the geostrophic wind to be more poorly related to the surface wind.

Scatter diagrams are presented in Fig. 7 for observed/geostrophic v components in Regions 1 (southwest) and 3 (north central). The slope is clearly less in Region 1 (Fig. 7a) than in Region 3 (Fig. 7b) (0.09 vs. 0.35), and the correlation coefficient is also much less (0.32 vs. 0.66). Although these differences are related to the different character of the terrain in the two regions, the range of geostrophic winds in Region 1 is unrealistically large (-40 m s^{-1} to $+40$ m s^{-1}). This indicates that the reduction errors also contribute significantly to the low correlation coefficients and slopes in Region 1, even when the MAPS SLP reduction is used, which has the best performance in this region.

It is notable that correlations and slopes are approximately equal for u and v components in all regions except for Region 1 (southwestern United States, Fig. 2a, 2b). In Region 1, v correlations tend to be higher for all four seasons and at both times of day for which data were collected. A possible explanation for this difference is related to the fact that terrain features in Region 1 (southwest) tend to be more oriented in the north–south direction (east–west standard deviation larger than that in north–south direction) than in other regions. This orientation, shown in directionally dependent terrain standard deviations for north–south and east–west directions relative to the grid (Fig. 8a and 8b), channels surface flow preferentially. This suggests that directionally dependent subgrid roughness lengths may be quite important for numerical models to forecast surface flow and terrain effects on flow.

e. Rotation angle variations

Correlations and slopes were calculated for nine different rotation angles. In the north central region (Region 3) where the highest correlations and slopes were found in general, the correlation coefficient maximized at a rotation angle of 35°–40° (Fig. 9). To eliminate the effect of weak flow on this statistic, only those cases were used in which observed winds were at least 10 knots (5.14 m s^{-1}) in magnitude. In the southwestern United States where terrain variations are much greater and a larger frictional component might be expected, the largest correlations were found at about 60° (figure not shown), using the same criteria. Pettersen (1969, p. 158) stated that rotation angles of 20°–25° with wind speeds of 60%-70% of geostrophic values may be expected over smooth grassland at anemometer level, and that angles of 45° with speeds 40% of geostrophic may be found over rough terrain. The statistics of this study give higher rotation angles and lower windspeed ratios than those suggested by Pettersen. Subsurface baroclinity effects from using sea level geostrophic winds instead of surface geostrophic winds in this study may account for some of this difference over Region 1 (southwest) but much less over Region 3 (north central) where the elevation is relatively low.

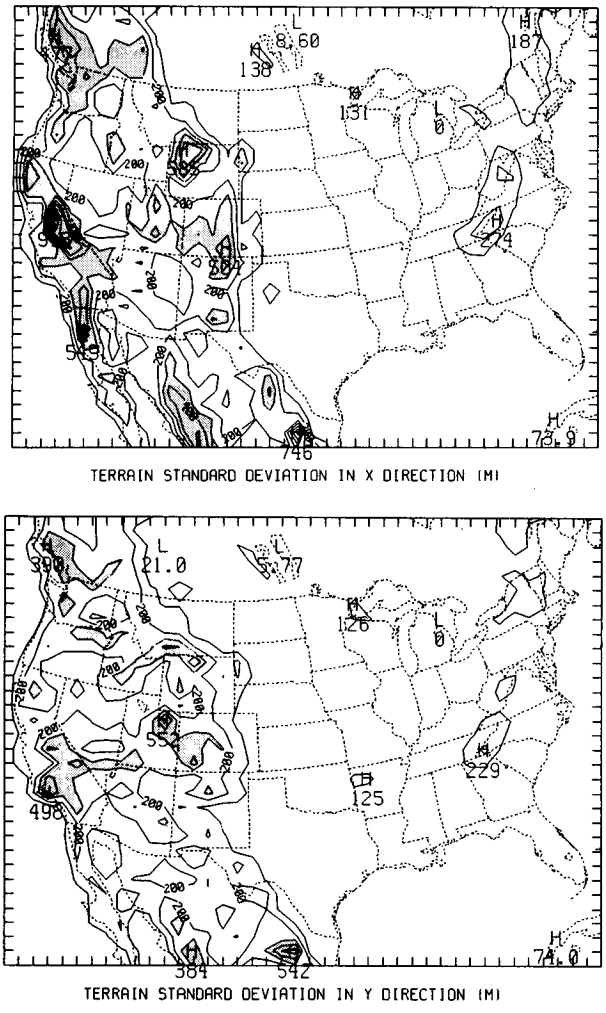

FIG. 8. Same as Fig. 5, but for directionally dependent elevation standard deviation from five-minute terrain data. a) east–west relative to grid, b) north–south relative to grid.

The drop-off of correlation on either side of the maximum was also lower than expected. Even at rotation angles of 100°, the correlations were about half that found at the maximum. This lack of drop-off is probably due, in part, to the large scatter in the data. It is a reflection of the fact that no single rotation angle is appropriate for all stations over an entire season. Schaefer and Doswell (1980) have analyzed the variation of rotation angle over a region at a single synoptic time in order to produce an antitriptic wind analysis. In this study, the correlation coefficients obtained for a single station (Kansas City, Missouri—MKC) are slightly higher than those for the entire population for the north central region (Fig. 9). The rotation angle with largest correlation cofficient for MKC was 45° (calculations done at 5° increments for this station), a larger angle than expected for a relatively flat region.

f. Dependence on wind speed

Correlation coefficients and slopes of regression were recalculated using only data pairs for observed winds > 5.14 m s^{-1} (10 knots). The correlation coefficients were about 0.1–0.2 higher for stronger winds than for the entire population and were as high as 0.9 for Region 3 (north central United States) at 0000 UTC. The slopes were also significantly higher, up to 0.5. These increases were consistent with the hypothesis that the correlation is dependent on the Froude number. In weaker wind situations, local circulations become more dominant, and the observed wind is much less dependent on the larger-scale pressure gradient. This is demonstrated in Fig. 10, comparing scatter diagrams for the observed/geostrophic wind pairs as weaker winds are excluded. Below 5.14 m s^{-1} (10 knots) in this region (southwestern United States), the geostrophic winds are not often useful predictors of the observed wind when the rotation angle is fixed (in this case, at 45°) over all stations and times. Both the correlation coefficient (0.44–0.60) and slope (0.21–0.60) increase as winds less than 7.7 m s^{-1} (15 knots) are excluded from the sample.

When only observed winds greater than 5.14 m s^{-1} (10 knots) were used (no figure shown), the MAPS SLP reduction again showed superiority to other reductions in Region 1 (southwestern United States),

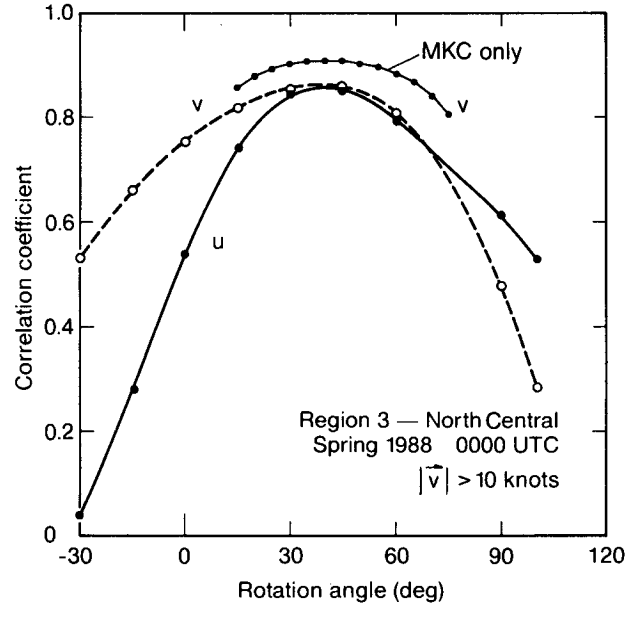

FIG. 9. Rotation angle dependence for correlation of MAPS SLP geostrophic wind versus observed wind for observed winds > 5.14 m s^{-1} (10 knots) in Region 3—north central United States. Solid line is for u component and dashed line is for v component. A second dashed line for the v component at Kansas City, MO (MKC) only is also shown.

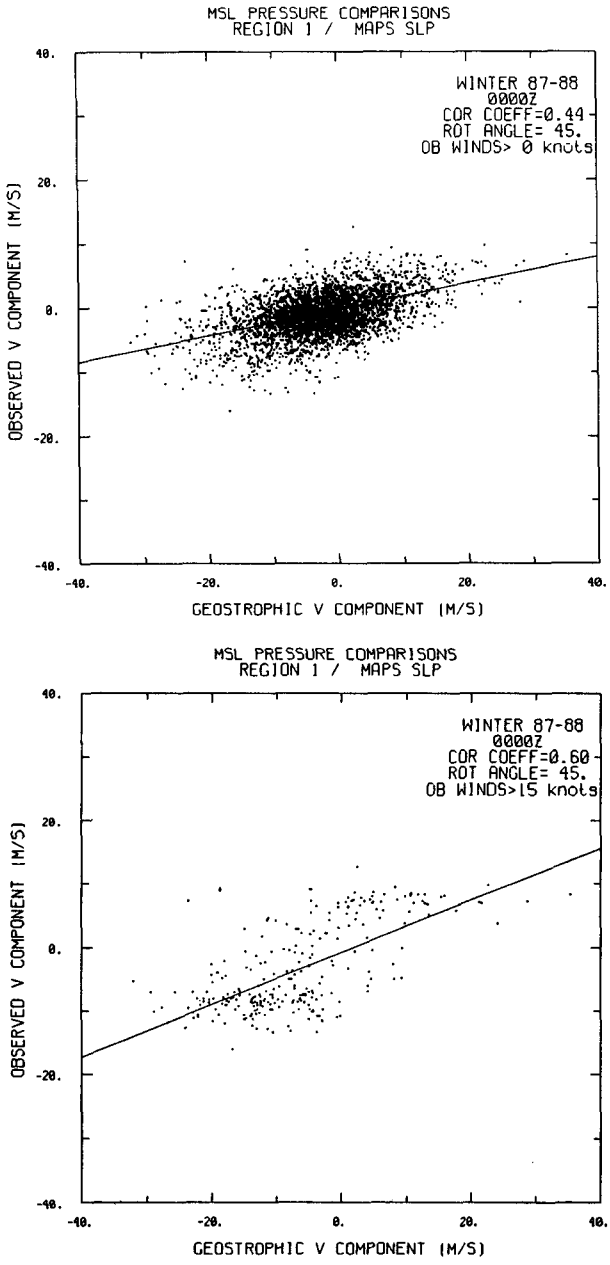

FIG. 10. Scatter diagrams for observed/geostrophic wind pairs of v component, MAPS SLP, Region 1 (southwest), winter 1988, 0000 UTC, rotation angle of 45°. a) all winds, b) observed winds > 7.7 m s^{-1} (15 knots) only.

but there was no significant difference in other regions, the same as the result from using the entire population.

g. Comparisons with the Sangster geostrophic wind

A comparison was made between geostrophic winds derived from station pressure reductions and those from the technique described by Sangster (1960, 1987) over a 31-day period in August–September 1989. The terrain used was the minimum topography field (Miller and Benjamin 1988) with a 2-pass smoother/desmoother (Shuman 1970). As suggested by Davies-Jones (1988), the solution for the Sangster potential field was determined with boundary values set equal to zero.

A comparison between the MAPS SLP and Sangster geostrophic winds (Table 2) shows that their performances are very close in Regions 2, 3, and 5. The Sangster method is slightly better in Region 1 and MAPS SLP is slightly better in Region 4. Both methods show substantial improvements over the standard SLP reduction in the western United States especially in Region 1, but there is little difference elsewhere. The ALT reduction gives the least correspondence between geostrophic wind estimates and observed winds in all five regions for this particular time period. The optimal angle of rotation (giving highest correlation coefficient) for both Sangster and MAPS SLP geostrophic winds was about 45° for all five geographical regions in this comparison.

5. Case study comparison between conventional SLP and MAPS SLP

A case study for 1 September 1989 is presented as an example of a situation over the western United States where MAPS SLP provided a more coherent picture of the synoptic pattern than the standard SLP analysis. The differences between reductions in this case are typical and not exceptional compared with those on other days, in our judgment. All analyses shown for this case are produced by an 80-km version of the analysis package described in Miller and Benjamin (1988); the Sangster geostrophic winds were calculated on an 111-km grid. The regional fields shown are extracted from analyses originally calculated over the entire conterminous United States and adjacent areas.

In this case, a cold front was moving southward across the plains from southern Minnesota to eastern Colorado. The surface potential temperature analysis

TABLE 2. Maximum correlation coefficients over rotation angle at 0000 UTC for period 7 August–6 September 1989. Values are for mean of u and v components, and bold type indicates maximum correlation for the region.

Region	Sangster	MAPS SLP	Std SLP	ALT
1	**0.48**	0.43	0.34	0.12
2	**0.47**	**0.47**	0.45	0.35
3	**0.74**	**0.74**	0.71	0.67
4	0.68	**0.72**	0.71	0.67
5	0.58	0.60	**0.61**	0.43

at 0200 UTC (Fig. 11a) over the region shows the potentially coolest air to the north of this front and the potentially warmest air over the higher terrain areas of Colorado, Arizona, and New Mexico. The main frontal zone appears split west of Wyoming; one gradient zone extends west through northern Utah and the other extends northwest toward Montana and Alberta.

The MAPS SLP, standard SLP, and altimeter setting analyses for this time are shown in Figs. 11b–d, and may be compared with the surface wind analysis and Sangster geostrophic winds in Figs. 11e–f. The main difference between the MAPS SLP (Fig. 11b) and standard SLP (Fig. 11c) analyses is in the alternating high and low pressure centers over western Colorado, Utah, Arizona and New Mexico. The MAPS SLP analysis shows a pressure gradient supporting the observed westerly flow over New Mexico unlike the standard SLP or altimeter analyses. The MAPS SLP analysis also shows a flatter gradient to the west where the other analyses showed much stronger alternating high/low center. The flatter gradient in the MAPS reduction is a result of using the 700 hPa temperature to lessen anomalies caused by the surface temperature. The Sangster geostrophic winds (Fig. 11f) are also well behaved in this area (i.e., light), but show regions of strong northerly geostrophic winds in southeastern Colorado and Nevada that do not appear to be consistent with observed winds.

Comparisons of reductions may also be made for neighboring stations. For instance, Colorado Springs (C) and Pueblo (P) in Colorado differ by 0.8 hPa in the MAPS SLP, 2.1 hPa in the standard SLP, and 4.1 hPa in altimeter setting. Similarly, Prescott (P) and Flagstaff (F) in Arizona differ by 0.4 hPa in MAPS SLP, 2.4 hPa in standard SLP, and 4.8 hPa in altimeter setting. Smaller differences between reduced pressure at neighboring stations are desirable. These comparisons show that the smoothing of the analysis masks some of the inaccuracies in the standard SLP and altimeter reductions.

Overall, results for the case study are consistent with the statistical results in that the altimeter setting should not be used over mountainous terrain (See Fujita 1989, for more examples of this) and in that the MAPS SLP reduction improves over the standard SLP reduction because it does not use the observed surface temperature.

6. Discussion and conclusions

A basic goal in sea level pressure reduction is to use a surface temperature which is representative of the free atmosphere and minimizes the introduction of fictitious baroclinity beneath the surface. A reduction based on the 700 hPa temperature (MAPS SLP) is presented to attempt to improve upon the standard SLP reduction over higher terrain regions. The MAPS SLP reduction uses the 700 hPa temperature with a standard lapse rate to define a "new" surface temperature at a station. The observed station pressure, derived from the altimeter setting, can than be reduced to sea level using the "new" surface temperature and a standard lapse rate. The estimate of representative surface temperature is the main difference between the MAPS SLP, standard SLP and altimeter reductions.

Since the *true* horizontal pressure gradient at the surface cannot be ascertained (Doswell 1988), a 21-month collection of observations over the contiguous United States has been used to assess the accuracy of different reductions by correlating their geostrophic winds with observed winds. Despite the considerable ageostrophic influences on surface winds, especially from terrain-related effects, surface wind observations are related strongly enough to the sea level pressure gradient that they can be used to provide independent verification. The results presented here show statistically how that relationship between observed surface winds and geostrophic wind estimates is dependent on the local stability, wind speed, and terrain variations; all of which are factors in the Froude number. These findings are consistent with theoretical studies (e.g., Pierrehumbert 1986) showing that blocking effects from terrain are dependent on the Froude number. If local terrain effects are strong, the statistical effect over a large number of such cases is that the correlation between observed wind and geostrophic wind becomes very small for all reductions and no particular reduction is shown to be advantageous. This result implies that the local Froude number could be used in a multivariate (wind/mass) objective analysis to estimate the degree of geostrophic coupling which should be assigned to low-level wind or pressure observations.

According to statistical comparisons with observed winds and subjective case studies (one of which is shown here), the MAPS SLP reduction is an improvement over the standard SLP reduction in the western United States. Over flatter, low elevation regions of the United States, differences in statistical performance for the various reductions are relatively small. Analyses using the altimeter setting reduction were generally the least accurate, especially in higher elevation regions. (Of course, the station pressure, uniquely defined by the altimeter setting and station elevation, is necessary to perform other reductions.) A statistical comparison for a 1-month data set using the Sangster geostrophic wind shows that the Sangster method and MAPS SLP perform similarly.

The Sangster method does not reduce surface pressue to sea level pressure at individual stations. Nevertheless, it is influenced by surface temperature, as pointed out by Sangster (1987) and Doswell (1988). Because of this influence, the Sangster method can produce large changes in surface geostrophic wind over sloping terrain without a change in actual surface pressure (Doswell 1988). The MAPS SLP reduction is immune to such a problem if the 700 hPa temperature remains un-

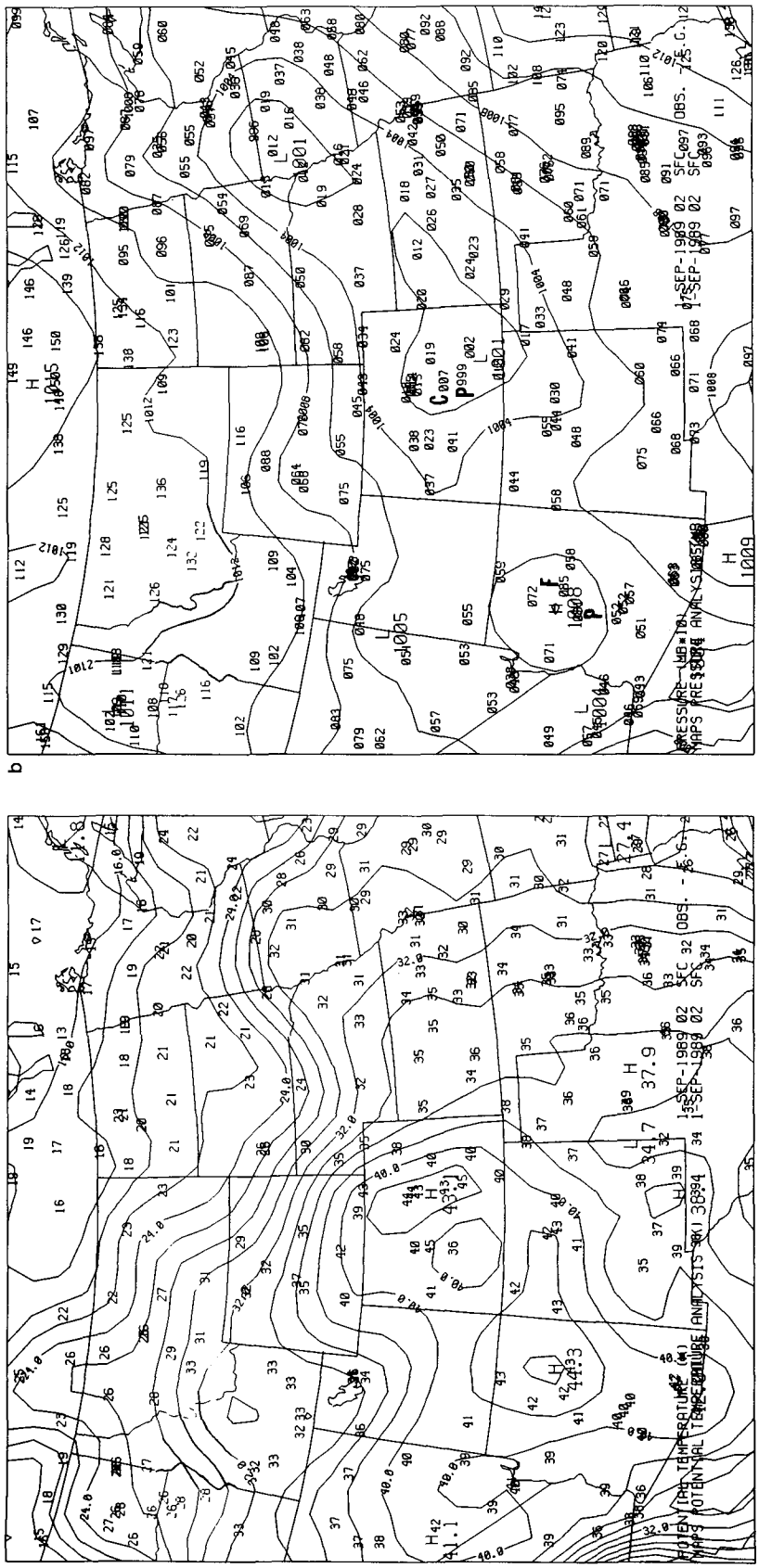

FIG. 11. Surface analyses with plotted observations for 0200 UTC 1 September 1989. (a) potential temperature (°C), (b) MAPS SLP (hPa).

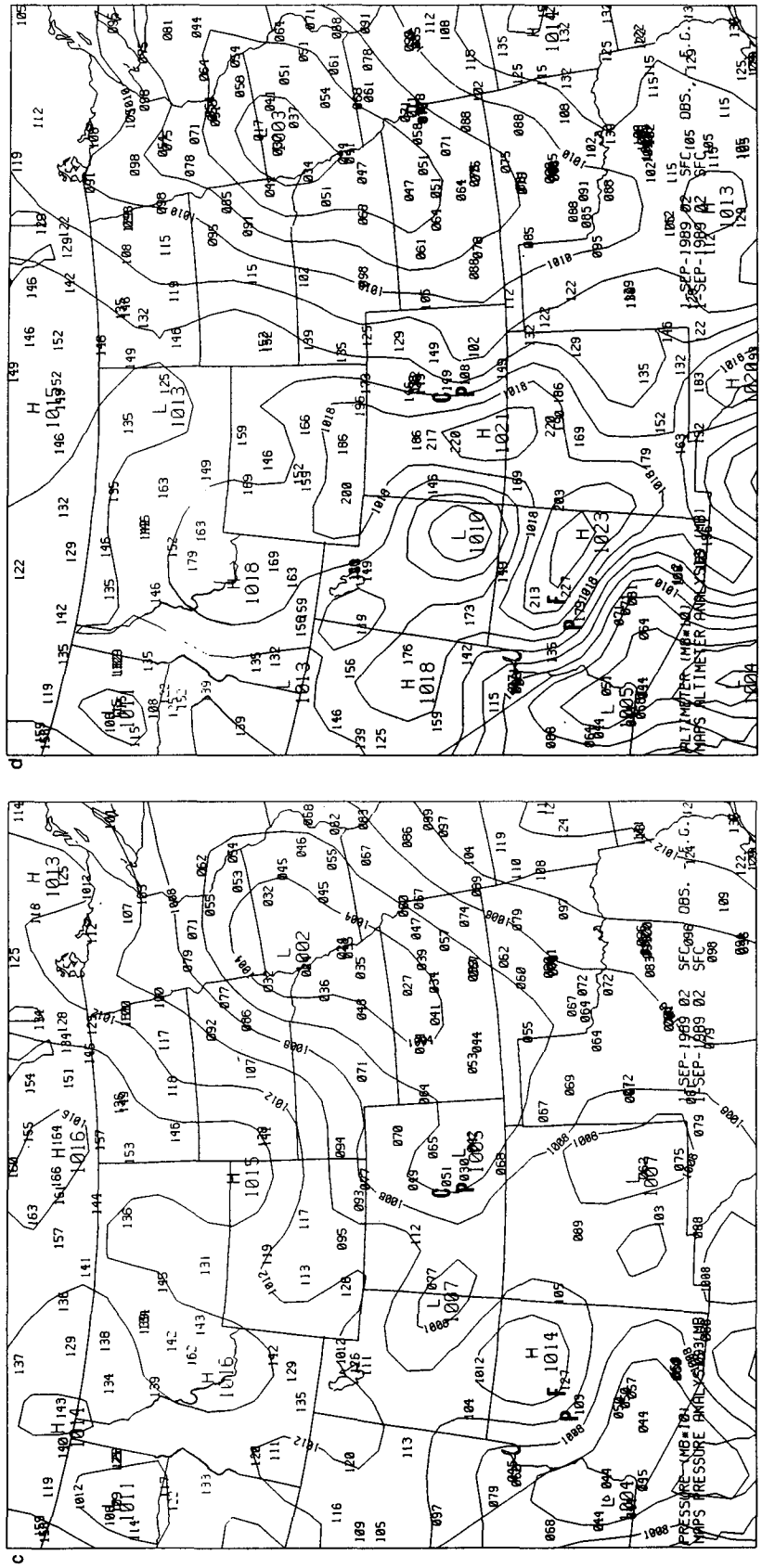

FIG. 11. (*Continued*) (c) standard SLP (hPa), (d) ALT (hPa).

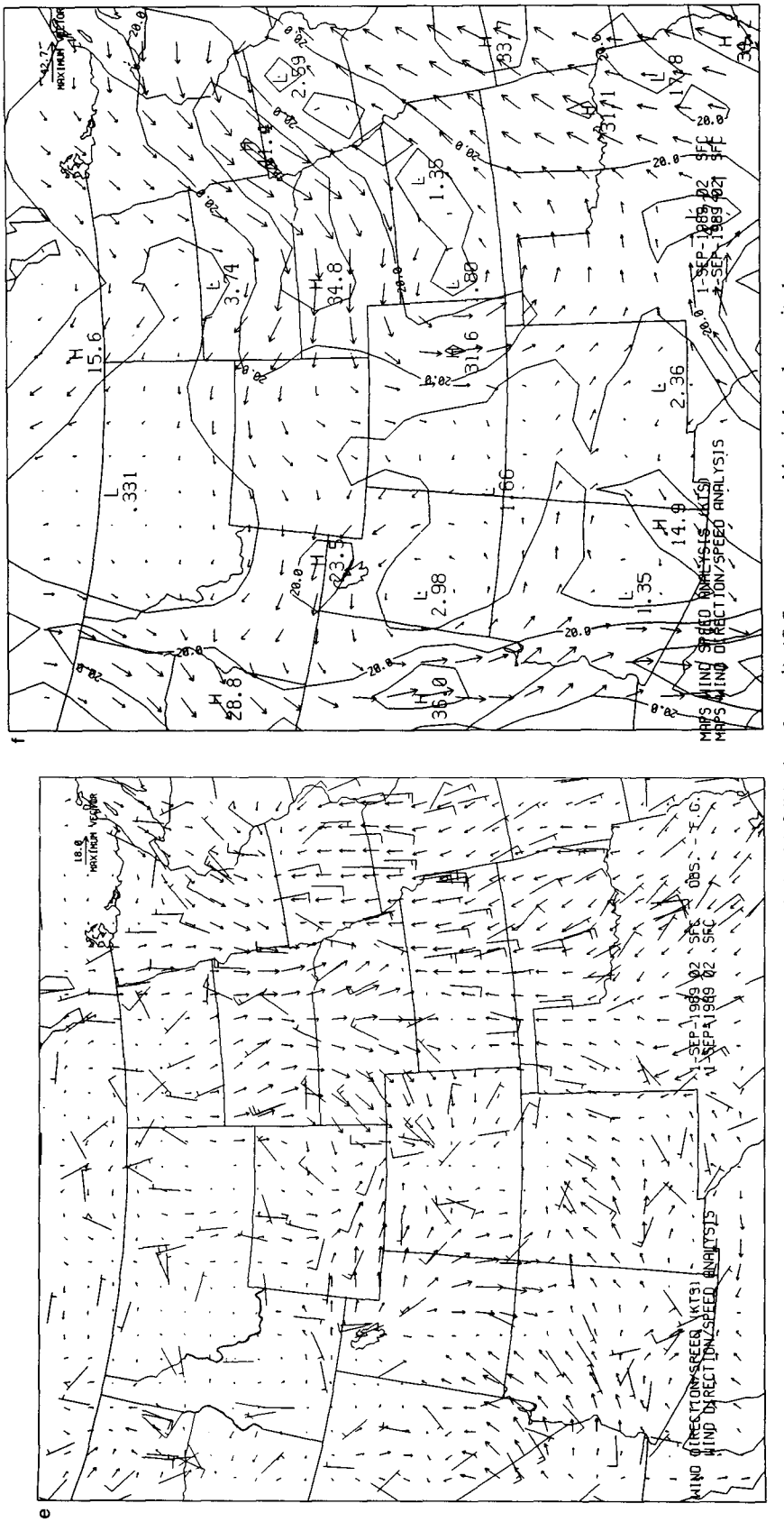

FIG. 11. (*Continued*) (e) winds (observed winds with full barb = 5 m s^{-1}), (f) Sangster geostrophic winds and magnitude.

changed. Also, the use of a station reduction allows the use of any desired analysis scheme as opposed to the Laplace equation solution required for the Sangster method.

On the other hand, some error can be produced in the MAPS SLP reduction from the 700 hPa temperature gradient. For instance, a nonzero sea level pressure gradient will be produced between two stations with equal elevation and equal surface pressure but with different 700 hPa temperatures. Also, 700 hPa temperatures are not actually free of diurnal influence over high terrain regions such as the western United States. If temperatures on terrain-following coordinates were available at, for instance, 200 hPa above the surface, using these temperatures might be preferable to using the 700 hPa temperature as done in the MAPS SLP reduction.

The Froude number effect on correlations between observed winds and geostrohic wind estimates was evident in statistical breakdowns by season (higher correlations in cooler seasons), time of day (higher at 0000 UTC than at 1200 UTC over the United States), region (higher in flatter areas of the United States), and wind speed (higher correlations with higher wind speeds). Maximum correlations occurred with relatively large rotational angles to account for friction: near 45° in flat areas and close to 60° in more mountainous regions (where subsurface baroclinity has a larger effect on sea level geostrophic winds).

MAPS surface analyses have been available on the PROFS workstation at the Denver National Weather Service Forecast Office since late 1986 and have been used with increasing frequency as forecasters have become familiar with them (Heideman et al. 1989). The MAPS SLP analysis has been the most commonly used among the surface analyses (standard SLP and Sangster surface geostrophic wind analyses are both also available), and forecasters at Denver have found that the MAPS SLP reduction provides a more representative field of surface pressure gradient than the standard SLP reduction (L. Dunn, personal communication).

Overall, the evidence presented here shows that, despite its imperfections, the MAPS SLP reduction improves over other station reduction methods in high terrain regions, apparently, because of the use of the 700 hPa temperature to estimate a more representative "surface" temperature.

Acknowledgments. We thank Charles Doswell—NSSL, Lawrence Dunn—NWS—Western Region, Denice Walker—NOAA/FSL, and two anonymous reviewers for their suggestions to improve this paper. We thank Jeff Smith of PROFS for helping us use his software for the Sangster geostrophic wind. The systems operations staff at PROFS made our work much easier in accessing the large amounts of data needed for this study. Nelson Seaman at Penn State University and the first author originally developed the idea of using 700 hPa temperatures for sea level pressure reduction, in that case, for model gridded data rather than for observations. Lindsay Murdock and Tom Schlatter of NOAA did an excellent job of editing manuscript drafts.

REFERENCES

Cram, J. M., and R. A. Pielke, 1989: Further comparison of two synoptic surface wind and pressure analysis methods. *Mon. Wea. Rev.*, **117**, 696–706.

Danard, J., 1989: On computing the surface horizontal pressure gradient over elevated terrain. *Mon. Wea. Rev.*, **117**, 1344–1350.

Davies-Jones, R., 1988: On the formulation of surface geostrophic streamfunction. *Mon. Wea. Rev.*, **116**, 1824–1826.

Doswell, C. A., 1988: Comments on "An improved technique for computing the horizontal pressure-gradient force at the earth's surface." *Mon. Wea. Rev.*, **116**, 1251–1254.

Fujita, T. T., 1989: The Teton-Yellowstone tornado of 21 July 1987. *Mon. Wea. Rev.*, **117**, 1912–1940.

Gandin, L. S., 1963: *Objective Analysis of Meteorological Fields.* Gidrometeorologicheskoe Izdatel'stvo, Leningrad. Translated from Russian, 1965, Israel Program for Scientific Translations, Jerusalem, Israel, 242 pp.

Garratt, J. R., 1984: Some aspects of mesoscale pressure field analysis. *Aust. Meteor. Mag.*, **32**, 115–122.

Gill, A. E., 1982: *Atmosphere-Ocean Dynamics.* Academic Press, 662 pp.

Heideman, K., D. Walker and J. A. Flueck, 1989: DAR^{3}E-I Evaluation: An Overview. NOAA Tech. Rep., ERL, NTIS 436-FSL 2, 29 pp.

Manual of Barometry (WBAN), 1963: Federal Meteorological Handbook No. 7, U.S. Government Printing Office, Washington, DC. [Available from NOAA/National Weather Service, Washington, DC 20233]

Mass, C. F., and D. P. Dempsey, 1985: A one-level, mesoscale model for diagnosing surface winds in mountainous and coastal regions. *Mon. Wea. Rev.*, **113**, 1211–1227.

McGinley, J. A., 1984: Scaling and theoretical considerations in variational analysis of flow around mountains. *Beitr. Phys. Atmos.*, **57**, 527–535.

Miller, P. A., and S. G. Benjamin, 1988: A scheme for analyzing surface observations over heterogeneous terrain. *Eighth Conf. Numerical Wea. Prediction*, Baltimore, Amer. Meteor. Soc., 178–184.

Pettersen, S., 1969: *Introduction to Meteorology*, McGraw-Hill, 333 pp.

Pielke, R. A., and J. M. Cram, 1987: An alternate procedure for analyzing surface geostrophic winds and pressure over elevated terrain. *Weather and Forecasting*, **2**, 229–236.

Pierrehumbert, R. T., 1986: Lee cyclogenesis. *Mesoscale Meteorology and Forecasting*, P. S. Ray, Ed. Amer. Meteor. Soc., 493–515.

Sangster, W. E., 1960: A method of representing the horizontal pressure gradient force without reduction of station pressure to sea level. *J. Meteor.*, **17**, 166–176.

——, 1987: An improved technique for computing the horizontal pressure-gradient force at the earth's surface. *Mon. Wea. Rev.*, **115**, 1358–1369.

Schaefer, J. T., and C. A. Doswell, 1980: The theory and practical application of antitriptic balance. *Mon. Wea. Rev.*, **108**, 746–756.

Saucier, W. J., 1955: *Principles of Meteorological Analysis.* The University of Chicago Press, 438 pp.

Shuman, R., 1970: Smoothing, filtering, and boundary effects. *Rev. Geophys. Space Phys.*, **8**, 359–387.

Wallace, J. M., and P. V. Hobbs, 1977: *Atmospheric Science*, Academic Press, 464 pp.